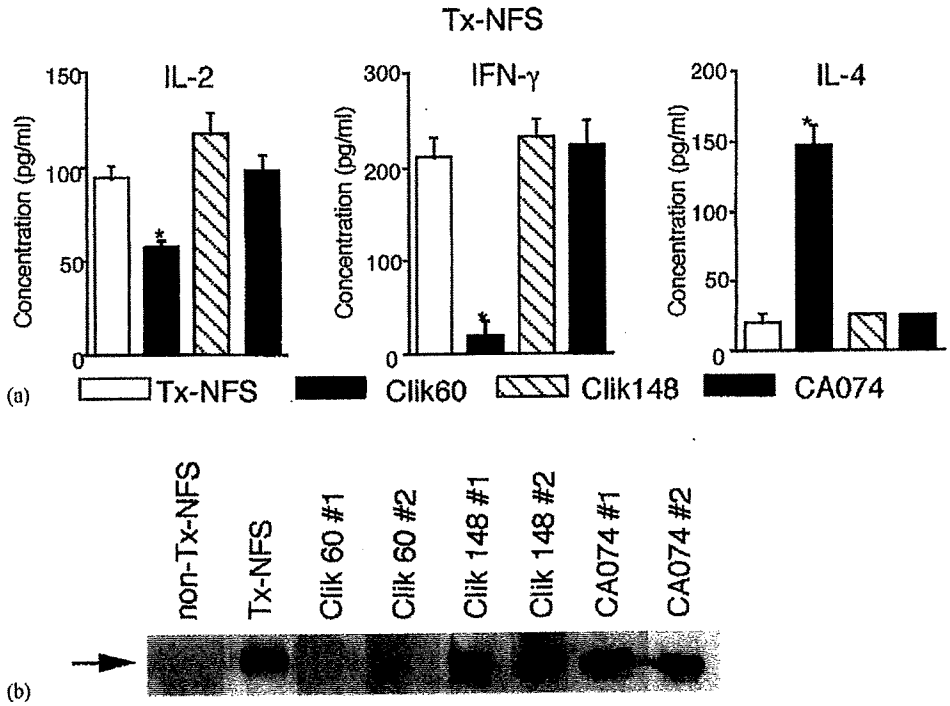

Fig. 3. (a) Down-regulation of the Th1-type cytokine production in the SS model mice treated with Clik60. Culture supernatants from anti-CD3 mAb-stimulated splenic T cells from Clik60-treated model mice (8-week-old) contained a high level of IL-4, but low levels of IL-2 and IFN-γ as measured by ELISA ($^{*}P<0.005$ and $^{**}P<0.001$, Student's t-test). (b) Inhibition of serum autoantibody production to 120 kD α-fodrin was observed in two different recipient mice treated with Clik60 (#1, #2) as shown by immunoblotting. Part of this Figure included in reference by Saegusa et al. (2002).

epithelial cells may function, at least in part, as autoantigen-presenting cells on the development of murine SS, and that inhibition of cathepsin S prevents the autoantigen presentation and subsequent peptide binding by class II molecules. MHC class II molecules bind a diverse array of peptides derived from the endocytic pathway and present them to $CD4^{+}$ T cells. MHC class II molecules are synthesized with their peptide-binding site blocked by Ii, and they acquire the capacity to bind antigens only after Ii has been degraded in the compartments. The treatment with cathepsin S-inhibitor was effective in preventing the development of autoimmune lesions in the SS model mice. In addition, Clik60-treated mice showed a significant downregulation of autoantigen (JS-1)-specific T cell response and Th1 cytokine expressions. These results indicate that cathepsin S-inhibitor plays an important role for preventing autoantigen presentation that followed by inhibition of autoimme exocrinopathy in SS.

Therapeutic effects of specific inhibitors of Cathepsin L (Clik148) for Autoimmune Diabetes (NOD) mice

We next examined the in vivo therapeutic effects of Clik60, Clik148, and CA074 in NOD mice, a well-known strain of animal model for autoimmune diabetes. Treatment with i.p. injection of Clik148 (0.1 mg/mouse/day) was effective in preventing the glucose production in blood and urine from the cychrophosphamide (CY)-treated NOD mice, but not in groups injected with CA074, and Clik60 (0.1 mg/mouse/day) (Fig. 4). To ensure the role of autoantigen-reactive T cells, we examined the proliferative T cell responses in the peripancreatic LNCs and spleen cells from CY-NOD mice and C57BL/6 control mice. We found that the peripancreatic LNCs and spleen cells in CY-NOD mice showed a significant increase in autoantigen (GAD and insulin)-specific T cell proliferation, but not in control mice. No significant differences were observed in the proliferative response stimulated with OVA (10 μg/ml) and ConA (5 μg/ml) among these mice. Then, we examined the inhibitory effects of cathepsin inhibitors against autoantigen-specific T cell responses in vitro. In peripancreatic LNCs from CY-NOD mice, a significantly inhibitory effect of Clik148 was observed in both anti-GAD and anti-insulin T cell responses, but no effects were found in incubation with Clik60 or CA074 (Fig. 5). Moreover, surface expressions of class II molecule induced by IFN-γ, and TNF-α stimulation in mouse islet β-cell line (Min6) was clearly inhibited by the incubation with Clik148, but not with Clik60 and CA074 determined by flow cytometry (Fig. 6). From these results, it was strongly suggested that Clik148 play a significant role in preventing autoantigen presentation to generate class II molecules competent for binding antigenic peptide, resulting in inhibition of autoimmune diabetes in NOD mice.

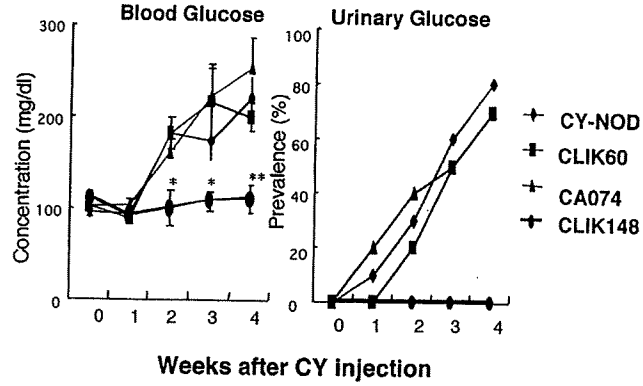

Fig. 4. Treatment with i.p. injection of Clik148 (0.1 mg/mouse/day) was effective in preventing the secretion of blood glucose and urine glucose from the cychrophosphamide (CY)-treated NOD mice ($^{*}P<0.05$, $^{**}P<0.01$, Student's t-test). The blood glucose level was monitored weekly with a glucometer using 50 μl blood from tail vein, and urine glucose was monitored with Keto-Diastix.

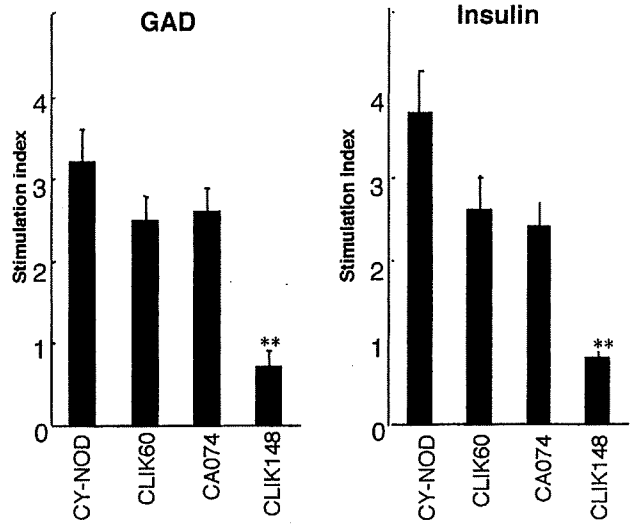

Fig. 5. Autoantigen (GAD and insulin)-stimulated proliferative T cell response of peripancreatic LNCs from NOD mice was significantly inhibited by incubation with Clik148, but not with Clik60, and CA074 (**$P<0.01$, Student's t-test). Data are expressed as stimulation indices (SI)±standard error of the mean (s.e.m.). Three experiments from each group were performed.

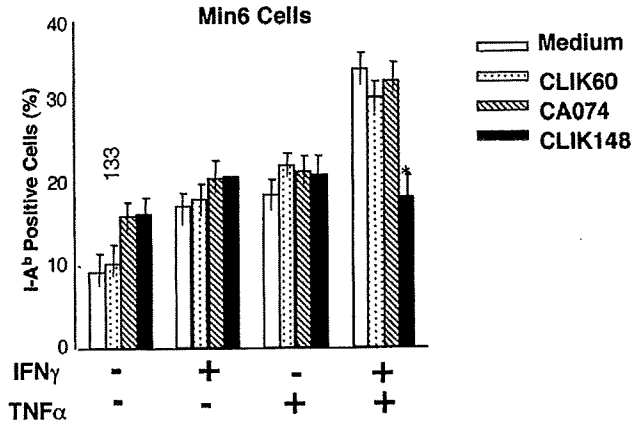

Fig. 6. Expression of MHC class II molecule induced by IFN-γ (100 U/ml), and TNF-α (100 U/ml)-stimulation in mouse islet β-cell line (Min6) was significantly inhibited by the treatment with Clik148, but not with Clik60, and CA074 (**$P<0.01$, Student's t-test). Three experiments from each group were performed.

Differential effect of cathepsin S and L on Antigen presentation

Recent studies have shown that cathepsin S and cathepsin L are important for Ag presentation by discrete populations of cells (Nakagawa et al., 1998, 1999; Shi et al.,

1999). Active cathepsin S was detected in B cells, dendritic cells (DCs), and peritoneal macrophages, where it was shown to be involved in the late stages of Ii degradation (Shi et al., 1999). By contrast, cathepsin L was detected only in macrophages and cortical thymic epithelial cells, where a defect resulted in severely impaired $CD4^+$ T cell selection (Nakagawa et al., 1998). Thus, it would appear that different APCs utilize distinct cathepsins to mediate late stage Ii degradation and regulate MHC class II presentation. Moreover, cathepsin S-deficient mice showed diminished susceptibility to collagen-induced arthritis, suggesting a potential therapeutic target for regulation of immune responsiveness (Nakagawa et al., 1999). Because of this cell type-restricted expression, cathepsin L deficiency results in diminished positive selection of $CD4^+$ T cells but does not significantly affect Ag presentation by bone marrow-derived APCs (Nakagawa et al., 1998). In contrast to Ii degradation, little is known about Ag processing, i.e., the proteolytic mechanisms that generate particular T cell epitopes. Early studies found that inhibition of lysosomal acidification interferes with proteolysis and Ag presentation, implicating lysosomal proteases (Watts, 1997). Evaluation of cathepsin L and cathepsin S has focused on their roles in Ii degradation and not in Ag processing (Villadangos and Ploegh, 2000). Recent evidence has demonstrated that several cathepsins are expressed in a tissue-specific fashion and that partial proteolysis of specific biological targets is a key function of cathepsins in antigen processing. We confirmed that mouse salivary gland cells and pancreas β islet cells might play an important role for presenting autopeptide in the autoimmune responses, and that inhibition of cathepsin S and cathepsin L prevents the surface expression of peptide/class II complex formation. The differential expression of proteinases by distinct APCs may affect the types of autoantigen peptides that are presented to T cells and thereby the immune responses that are ultimately generated. Our experiments support the hypothesis that cathepsin S, and cathepsin L, previously shown to be important in Ii processing in vitro, regulates MHC class II function and subsequent autoimmune responses in vivo. Thus, selective inhibition of cysteine proteases cathepsin S and cathepsin L may have important therapeutic potential in modulating class II–restricted autoimmune processes.

Summary

The cysteinal lysosomal proteases, cathepsin S and cathepsin L have been shown to process invariant chain, thereby facilitating MHC class II maturation. However, their role in antigen processing is not established. Studies examined the functional significance of cathepsin inhibition on antigen processing and autoimmune diseases in murine models for SS and non-obese type-I diabetes model (NOD). Specific inhibitor of cathepsin S (Clik60) in vitro markedly impaired presentation of an organ-specific autoantigen, 120 kD α-fodrin, by interfering with MHC class II–peptide binding. Antigen-specific T cell responses were significantly inhibited by incubation with Clik60 in dose-dependent manner. Ttreatment with Clik60 in vivo profoundly blocked lymphocytic infiltrations in the salivary and lacrimal glands and

abrogated a rise in serum autoantibody production. Moreover, treatment with i.p. injection of specific inhibitor of cathepsin L (Clik148) was effective in preventing the glucose production in blood and urine from NOD mice, but not in groups injected with CA074 and Clik60. Clik148 markedly impaired presentation of autoantigens including insulin and GAD in NOD mice. Thus, inhibition of cathepsin activity in vivo alters autoantigen presentation and development of autoimmunity. Our experiments demonstrate that selective inhibition of cysteine proteases is an additional potential strategy for modulating the autoantigen-derived immune response in class II—restricted autoimmune diseases including Sjögren's syndrome and autoimmune diabetes.

References

Bevec T, Stoka V, Pungercic G, Dolenc I, Turk V. Major histocompatibility complex class II-associated p41 invariant chain fragment is a strong inhibitor of lysosomal cathepsin L. J Exp Med 1996;183: 1331–8.

Chan EK, Hamel JC, Buyon JP, Tan ET. Molecular definition and sequence motifs of the 52-kD component of human SS-A/Ro autoantigen. J Clin Invest 1991;87:68–76.

Cresswell P. Antigen presentation. Getting peptides onto MHC class II molecules. Curr Biol 1994;4:541–3.

Delporte BC, Delporte C, O'Connell BC, He X, Lancaster HE, O'Connell AC, Agre P, Baum BJ. Increased fluid secretion after adenoviral-mediated transfer of the aquaporin-1 cDNA to irradiated rat salivary glands. Proc Nat Acad Sci 1997;94:3268–73.

Fox RI, Robinson CA, Curd JG, Kozin F, Howell FV. Sjögren's syndrome. Proposed criteria for classification. Arthritis Rheum 1986;29:577–85.

Germain RN. MHC-dependent antigen processing and peptide presentation: providing ligands for T lymphocyte activation. Cell 1994;76:287–99.

Haneji N, Hamano H, Yanagi K, Hayashi Y. A new animal model for primary Sjögren's syndrome in NFS/*sld* mutant mice. J Immunol 1994;153:2769–77.

Haneji N, Nakamura T, Takio K, Yanagi K, Higashiyama H, Saito I, Noji S, Sugino H, Hayashi Y. Identification of α-fodrin as a candidate autoantigen in primary Sjögren's syndrome. Science 1997;276:604–7.

Haskins K, McDuffie M. Acceleration of diabetes in young NOD mice with a CD4 islet-specific T cell clone. Science 1990;249:1433–6.

Hayashi Y, Kojima A, Hata M, Hirokawa K. A new mutation involving the sublingual gland in NFS/N mice: partially arrested mucous cell differentiation. Am J Pathol 1988;132:187–91.

Katunumua N, Murata E, Kakegawa H, Matsui A, Tsuzuki H, Tsuge H, Turk D, Turk V, Fukushima M, Tada Y, Asao T. Structure based development of novel specific inhibitors for cathepsin L and cathepsin S in vivo and in vitro. FEBS Lett 1999;458:6–10.

Katz JD, Wang B, Haskins K, Benoist C, Mathis D. Following a diabetogenic T cell from genesis through pathogenesis. Cell 1993;74:1089–100.

Kaufman DL, Clare-Salzier M, Tian J, Forsthuber T, Ting GSP, Robinson P, Atkinson MA, Sercarz EE, Tobin AJ, Lehmann OV. Spontaneous loss of T-cell tolerance to glutamic acid decarboxylase in murine insulin-dependent diabetes. Nature 1993;366:69–72.

Kruize AA, Smeenk RJT, Kater L. Diagnostic criteria and immunopathogenesis of Sjögren's syndrome: implications for therapy. Immunol Today 1995;16:557–9.

Lamb C, Cresswell P. Assembly and transport properties of invariant chain trimers and HLA-DR-invariant chain complexes. J Immunol 1992;148:3478–82.

Liu E, Moriyama H, Abiru N, Miano D, Yu L, Taylor RM, Finkelman FD, Eisenbarth GS. Anti-peptide autoantibodies and fetal anaphylaxis in NOD mice in response to insulin self-peptide B:9-23 and B:13-23. J Clin Invest 2002;110:1021–7.

Matsunaga Y, Saibara T, Kido H, Katunuma N. Participation of cathepsin B in processing of antigen presentation to MHC class II. FEBS Lett 1993;324:325–30.

Murata M, Miyashita S, Yokoo C, Tamai M, Hanada K, Hatayama K, Towatari T, Nikawa T, Katunuma N. Novel epoxysuccinyl peptides: selective inhibitors of cathepsin B, in vitro. FEBS Lett 1991;280:307–10.

Nakagawa T, Roth W, Wong P, Nelson A, Farr A, Deussing J, Villadangos JA, Ploegh H, Peters C, Rudensky AY. Cathepsin L: critical role in Ii degradation and CD4T cell selection in the thymus. Science 1998;280:450–3.

Nakagawa T, Brissette WH, Lira PD, Griffiths RJ, Petrushova N, Stock J, McNeish JD, Eastman SE, Howard ED, Clarke SR, Rosloniec EF, Elliott EA, Rudensky AY. Impaired invariant chain degradation and antigen presentation and diminished collagen-induced arthritis in cathepsin S null mice. Immunity 1999;10:207–17.

Reyes VE, Lu S, Humphreys RE. Cathepsin B cleavage of Ii from MHC α- and β-chains. J Immunol 1991;146:3877–80.

Roche PA, Marks MS, Cresswell P. Formation of a nine-subunit complex by HLA class II glycoproteins and the invariant chain. Nature 1991;354:392–4.

Saegusa K, Ishimaru N, Yanagi K, Arakaki R, Ogawa K, Saito I, Katunuma N, Hayashi Y. Cathepsin S inhibitor prevents autoantigen presentation and autoimmunity. J Clin Invest 2002;110:361–9.

Shi GP, Munger JS, Meara JP, Rich DH, Chapman HA. Molecular cloning and expression of human alveolar macrophage cathepsin S, an elastinolytic cysteine protease. J Biol Chem 1992;267:7258–62.

Shi GP, Webb AC, Foster KE, Knoll JHM, Lemere CA, Munger JS, Chapman HA. Human cathepsin S: chromosomal localization, gene structure, and tissue distribution. J Biol Chem 1994;269:11530–6.

Shi GP, Villadangos JA, Dranoff G, Small C, Gu L, Haley KJ, Riese R, Ploegh HL, Chapman HA. Cathepsin S required for normal MHC class II peptide loading and germinal center development. Immunity 1999;10:197–206.

Towatari T, Nikawa T, Murata M, Yokoo C, Tamai M, Hanada K, Katunuma N. Novel epoxysuccinyl peptides: a selective inhibitor of cathepsin B, in vivo. FEBS Lett 1991;280:311–5.

Villadangos JA, Ploegh HL. Proteolysis in MHC class II antigen presentation: who's in charge? Immunity 2000;12:233–9.

Watts C. Capture and processing of exogenous antigens for presentation on MHC molecules. Annu Rev Immunol 1997;15:821–50.

White SC, Caserett GW. Induction of experimental autoallergic sialadenitis. J Immunol 1974;112:178–85.

Wolf PR, Ploegh HL. How MHC class II molecules acquire peptide cargo: biosynthesis and trafficking through the endocytic pathway. Annu Rev Cell Dev Biol 1995;11:267–306.

ARTHRITIS & RHEUMATISM
Vol. 50, No. 9, September 2004, pp 2903–2910
DOI 10.1002/art.20472
© 2004, American College of Rheumatology

Effective Treatment of a Mouse Model of Sjögren's Syndrome With Eyedrop Administration of Anti-CD4 Monoclonal Antibody

Yuki Hayashi,[1] Naozumi Ishimaru,[2] Rieko Arakaki,[2] Shin-ichi Tsukumo,[1] Hitomi Fukui,[2] Kenji Kishihara,[1] Hiroshi Shiota,[1] Koji Yasutomo,[1] and Yoshio Hayashi[2]

Objective. **To determine whether eyedrop administration of an anti-CD4 monoclonal antibody (mAb) is effective in the treatment of Sjögren's syndrome (SS) using a mouse model of the disease.**

Methods. **The anti-CD4 mAb was administered daily into the eyes of mice with SS from ages 4 to 8 weeks or ages 10 to 12 weeks. During treatment, tear volume was monitored and after final treatment, histologic features of the lacrimal and salivary glands, the phenotypes and function of T cells, and serum titers of anti–α-fodrin antibody were examined.**

Results. **Eyedrop administration of anti-CD4 mAb before the onset of SS prevented the autoimmune pathology seen in the lacrimal glands but not that in the salivary glands. Furthermore, eyedrop administration of anti-CD4 mAb after the development of SS inhibited mononuclear cell infiltration and the destruction of parenchyma only in the lacrimal glands. Eyedrop administration of anti-CD4 mAb suppressed the local activation of CD4+ T cells rather than deleting CD4+ T cells, which reduced the expansion of pathologic CD4+ T cells against α-fodrin.**

Conclusion. **These results demonstrate the remarkable efficacy of anti-CD4 mAb eyedrops in the treatment of SS eye symptoms, which illustrates a new antibody-based therapeutic strategy for patients with eye problems caused by SS as well as other diseases.**

The immune system has acquired regulatory systems that preclude the reactivity of mature T cells against self antigens presented by major histocompatibility complex (MHC), while maintaining an ability to respond to non-self antigens presented by self MHC (1,2). The deletion of T cells that have T cell receptors with a high affinity for self antigens in the thymus is an important mechanism for self-tolerance induction and many other systems, including apoptosis, anergy of mature T cells and regulatory T cells, and control T cell tolerance (3–5). The dysregulation of T cell tolerance induction/maintenance is considered to be responsible for many types of autoimmune diseases, and a variety of mechanisms for causing autoimmune diseases have been proposed (5–9). However, the precise mechanisms of human autoimmune diseases remain unclear, and this prevents the establishment of specific therapeutic strategies for these conditions.

Sjögren's syndrome (SS) is an autoimmune disease characterized by the destruction of lacrimal and salivary glands, resulting in dry eyes and dry mouth as the major symptoms (10). Because SS patients have high titers of autoantibodies, including anti-SSA/Ro and SSB/La, abnormal T and B cell activation has been considered to cause SS (10,11). We have established and investigated an animal model of SS in NFS/*sld*-mutant mice thymectomized 3 days after birth and found that the 120-kd α-fodrin protein is a critical autoantigen in the development of SS in this mouse model (12–14). Furthermore, we and other investigators (12,15) have found that patients with SS have high titers of serum

Supported in part by Grants-in-Aid for Young Scientists (A) (15689016) from the Ministry of Education, Science, Technology, Sports, and Culture, Japan.

[1]Yuki Hayashi, MD, PhD, Shin-ichi Tsukumo, PhD, Kenji Kishihara, PhD, Hiroshi Shiota, MD, PhD, Koji Yasutomo, MD, PhD: The University of Tokushima School of Medicine, Tokushima, Japan; [2]Naozumi Ishimaru, DDS, PhD, Rieko Arakaki, PhD, Hitomi Fukui, Yoshio Hayashi, DDS, PhD: The University of Tokushima School of Dentistry, Tokushima, Japan.

Address correspondence and reprint requests to Koji Yasutomo, MD, PhD, Department of Immunology and Parasitology, School of Medicine, The University of Tokushima, 3-18-15 Kuramoto, Tokushima 770-8503, Japan. E-mail: yasutomo@basic.med.tokushima-u.ac.jp.

Submitted for publication January 9, 2004; accepted in revised form May 12, 2004.

anti–α-fodrin antibody, suggesting that α-fodrin is a critical autoantigen for the onset or progression of human SS. Although the mechanism of autoimmune disorders in the lacrimal and salivary glands in this mouse model is still unclear, autoreactive CD4+ T cells are responsible for the destruction of the lacrimal and salivary glands in this model (16–18) as well as in human SS (19,20).

Patients with SS are treated with oral or intravenous immunosuppressive drugs, including steroids and cyclosporin A (CSA), which suppress T cell proliferation (10). Such drugs are effective in certain SS patients, but sometimes induce severe side effects (10). The characteristic symptom of SS is dry eyes (10,21), so it is better to treat this symptom with eyedrop (ED) administration of drugs rather than systemically. In this regard, topical CSA has been successfully used as a treatment for the eye symptoms of SS (22), although double-blind clinical studies of SS patients are necessary for the final determination of its efficacy.

To establish a topical therapeutic strategy for the eye symptoms of SS patients, we evaluated ED administration of anti-CD4 monoclonal antibody (mAb) in a mouse model of SS. The anti-CD4 mAb specifically affects CD4+ T cell activation, the dysregulation of which is responsible for the development of SS symptoms in mice and humans (16–18). Although an antibody is a high molecular weight glycoprotein, we found that ED administration of anti-CD4 prevented the onset as well as the progression of autoimmune responses in the lacrimal glands in mice with SS by inhibiting CD4+ T cell activation, possibly through infiltration of the antibody into the lacrimal glands. These findings suggest that it might be possible to treat the eye symptoms of humans with SS as well as other diseases with ED administration of antibodies that recognize critical molecules that cause each disease.

MATERIALS AND METHODS

Mice and experimental protocol. Female NFS/*sld* mice carrying the mutant gene *sld* (23) were bred in our specific pathogen–free mouse colony and were provided with food and water ad libitum. A thymectomy was performed on NFS/*sld* mice 3 days after birth (3d-Tx mice), as previously described (12,24). For the eyedrops, 2 μl of anti-CD4 mAb (GK1.5) dissolved in phosphate buffered saline was prepared in our laboratory (1 mg/ml) and applied with a micropipette to both eyes once a day from 4 to 8 weeks of age or from 10 to 12 weeks of age. As a control, rat IgG eyedrops (Inter-Cell Technologies, Hopewell, NJ) were used.

Histologic examination. The mice were killed at 8 or 12 weeks of age. All organs were removed, fixed in 4% phosphate buffered formaldehyde (pH 7.2), and prepared for histologic examination. Sections were stained with hematoxylin and eosin (H&E). Histologic grading of inflammatory lesions was performed according to the method proposed by White and Casarett (25), as follows: 1 = 1–5 foci composed of >20 mononuclear cells per focus, 2 = >5 such foci, but without

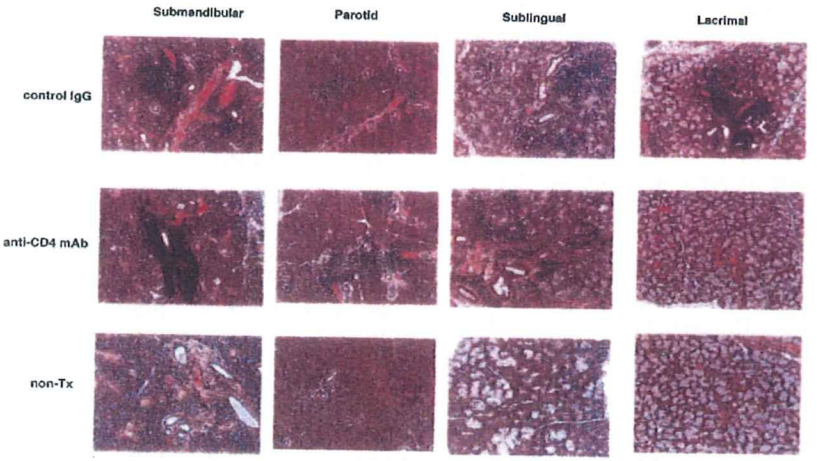

Figure 1. Suppression of autoimmune responses in lacrimal glands by treatment with eyedrop (ED) administration of CD4. Mice thymectomized 3 days after birth were treated with ED administration of control IgG or anti-CD4 monoclonal antibody (mAb) from ages 4 to 8 weeks. The lacrimal, parotid, submandibular, or sublingual glands were removed 4 weeks after initial treatment and stained with hematoxylin and eosin. As a control, nonthymectomized (non-Tx) NSF/*sld* mice were used. Results are representative of 4 independent experiments.

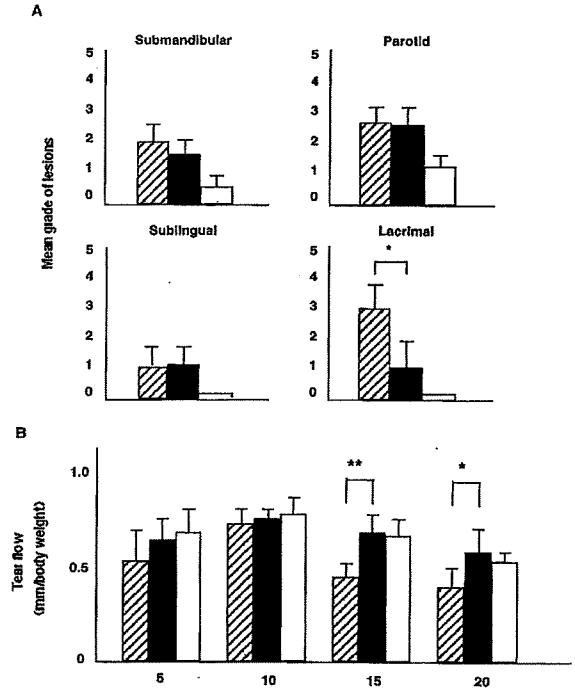

Figure 2. Prevention of the onset of autoimmune responses by ED administration of CD4 in lacrimal glands only. **A,** The 3-day-old thymectomized (3d-Tx) mice were treated with eyedrop (ED) administration of control IgG (hatched bars) or anti-CD4 mAb (solid bars) from ages 4 to 8 weeks. The lacrimal, parotid, submandibular, or sublingual glands were removed 4 weeks after initial treatment and stained with hematoxylin and eosin. As a control, nonthymectomized (non-Tx) NSF/*sld* mice were used (open bars). The histologic scores of each gland were evaluated as described in Materials and Methods. Values are the mean and SEM of 7 mice. * = $P < 0.01$. **B,** The 3d-Tx mice were treated with ED administration of control IgG (hatched bars) or anti-CD4 mAb (solid bars) from ages 4 to 8 weeks. As a control, non-Tx NSF/*sld* mice were used (open bars). The tear volume of each mouse was evaluated as described in Materials and Methods. Values are the mean and SEM of 9 mice. * = $P < 0.05$; ** = $P < 0.01$.

significant parenchymal destruction, 3 = degeneration of parenchymal tissue, 4 = extensive infiltration of the glands with mononuclear cells and extensive parenchymal destruction, and 5 = severe destructive foci with focal fibrosis, ductal dilation, and/or fatty infiltration in addition to the grade 4 lesions. Histologic evaluation of the lacrimal and salivary glands was performed in a blinded manner, and 1 tissue section from each lacrimal and salivary gland was examined.

Flow cytometric analysis. Single-cell suspensions from the lymph nodes or spleen were stained with a combination of phycoerythrin (PE)–conjugated anti-CD4 mAb and fluorescein isothiocyanate–conjugated anti-CD8 mAb or PE-conjugated anti-CD4 mAb and cytochrome-conjugated anti-CD44 mAb and analyzed with a FACSCalibur flow cytometer (Becton Dickinson, Mountain View, CA). Cells were gated according to size and scatter to eliminate dead cells and debris from analysis. All antibodies were from BD Transduction Laboratories (San Jose, CA).

Measurement of fluid secretion. Analysis of the tear and saliva volume of 15 treated and 15 untreated 3d-Tx NFS/*sld* mice and 12 non–3d-Tx NFS/*sld* mice was performed according to a previously described method (26). A total of 42 mice were examined.

Proliferation assay. Total spleen cells or cervical lymph node cells (5×10^5/well) in RPMI 1640 containing 10% fetal calf serum, penicillin/streptomycin, and 2-mercaptoethanol were stimulated with recombinant α-fodrin protein (JS-1) (12) or 2.0 μg/ml concanavalin A (Con A; Sigma, St. Louis, MO) in 96-well, flat-bottomed plates for 72 hours. Then, ^{3}H-thymidine (1 μCi/well; NEN Life Science Products, Boston, MA) was pulsed into the cell mixture during the final 20 hours of culture. Incorporation of ^{3}H-thymidine was evaluated by an automated β-liquid scintillation counter (MicroPlus; Wallace, Turku, Finland).

Enzyme-linked immunosorbent assay (ELISA). The 96-well plates were coated with JS-1 (12). After washing the protein, diluted serum from mice with SS was added. Biotinylated anti-mouse IgG (Vector, Burlingame, CA) was added as the second antibody. The JS-1–specific antibodies were measured by an automatic ELISA reader (Flow, McLean, VA).

Statistical analysis. The results of histologic, tear secretion, and flow cytometric analyses as well as proliferation assay and ELISA were evaluated by Student's *t*-test.

RESULTS

Prevention of the onset of autoimmune pathology in lacrimal glands by ED administration of CD4. The 3d-Tx NFS/*sld* mice began to develop autoimmune lesions in the lacrimal and salivary glands at 4 weeks of age or later, while no inflammatory lesions were observed in non–3d-Tx NFS/*sld* mice (12). To evaluate whether ED administration of CD4 was effective for preventing the onset of SS autoimmune pathology, anti-CD4 mAb was applied daily to both eyes of 3d-Tx mice from 4 to 8 weeks of age. Then the histologic features of the lacrimal, parotid, submandibular, and sublingual glands of anti-CD4 mAb– or control IgG-treated mice were evaluated by H&E staining (Figures 1 and 2). The lacrimal, parotid, submandibular, and sublingual glands of control IgG-treated 3d-Tx mice showed massive infiltration of mononuclear cells around ducts, as well as destruction of parenchyma, 4 weeks after initial treatment (Figure 1).

In contrast, the infiltration of mononuclear cells as well as the destruction of parenchyma was inhibited in the lacrimal glands, but not the parotid, submandibular, and sublingual glands, of 3d-Tx mice treated with ED administration of CD4 (Figure 1). The non–3d-Tx NSF/*sld* mice did not develop any autoimmune responses

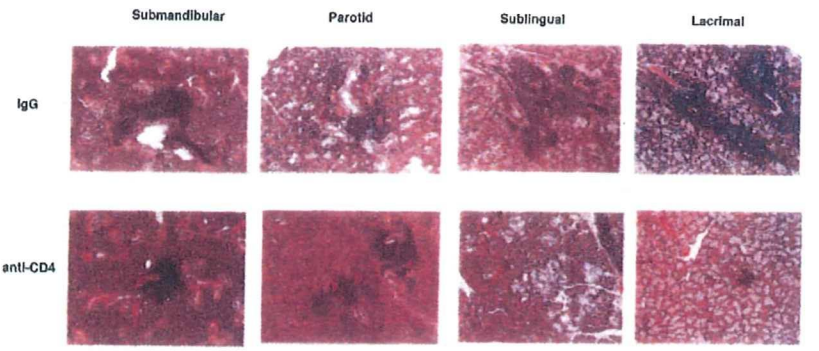

Figure 3. Suppression of established autoimmune responses in lacrimal glands by ED administration of CD4. The 3d-Tx mice were treated with ED administration of control IgG or anti-CD4 mAb from ages 10 to 12 weeks. The lacrimal, parotid, submandibular, or sublingual glands were removed 2 weeks after initial treatment and stained with hematoxylin and eosin. Results are representative of 3 independent experiments. See Figure 2 for definitions.

(Figure 1). Those histologic findings were scored 4 weeks after initial treatment, as described in Materials and Methods (Figure 2A). The 3d-Tx NFS/*sld* mice treated with ED administration of CD4 had significantly inhibited autoimmune responses only in the lacrimal glands ($P < 0.01$) (Figure 2A), although there were still very small foci of infiltrating mononuclear cells in the lacrimal glands. Furthermore, the average tear volume of mice treated with ED administration of CD4 significantly recovered to the level of control IgG-treated mice (Figure 2B). These results demonstrate that ED administration of CD4 specifically suppressed the onset of autoimmune responses in the lacrimal glands, but not the salivary glands.

Suppression of already developed autoimmune pathology by ED administration of CD4. It is necessary to consider the clinical use of a therapeutic strategy and establish one that can suppress autoimmune pathology that has already developed. Thus, in order to examine the effect of ED administration of CD4 on the autoimmune lesions of mice that had already developed SS, we initiated treatment at 10 weeks of age and continued it for 2 weeks. Then, histologic sections of the lacrimal, parotid, submandibular, and sublingual glands were examined by H&E staining 2 weeks after initial treatment. ED administration of CD4 suppressed the cell infiltration and parenchyma destruction of the lacrimal glands, but not of the parotid, submandibular, or sublingual glands (Figure 3), similar to the therapeutic effects of ED administration of CD4 before the onset of autoimmune diseases (Figures 1 and 2). The histologic scores clearly demonstrated that the therapeutic effect is limited only to the lacrimal glands (Figure 4A), indicating that ED administration of CD4 also has the potential to suppress progression of already developed autoimmune diseases. In contrast, the tear volume of mice treated with ED administration of CD4 was not significantly increased compared with that of mice treated with control IgG (Figure 4B).

CD4+ T cell number augmented and activation inhibited by ED administration of CD4. The anti-CD4 mAb used can cause the deletion of CD4+ T cells when injected into mice and can block the interaction between CD4 and class II MHC (27,28). Thus, we next examined whether the therapeutic effect of ED administration of CD4 on 3d-Tx NFS/*sld* mice was attributable to the deletion of CD4+ T cells or the inhibition of CD4+ T cell activation.

Cervical lymph node cells and spleen cells were purified from 3d-Tx NFS/*sld* mice treated with ED administration of CD4 from 4 to 8 weeks of age or 10 to 12 weeks of age. In mice treated from 4 to 8 weeks of age, the relative number of CD4+ T cells from lymph nodes was increased compared with the number of CD8+ T cells and compared with the control IgG-treated group (Figure 5A). Since the total cell number did not change with ED administration of CD4 (Figure 5A), only the total CD4+ T cells and not the CD8+ T cells increased. The relative and total numbers of both CD4+ and CD8+ T cells from lymph nodes were increased in mice treated with ED administration of CD4 from 10 to 12 weeks of age (Figure 5B). In contrast, the number of CD4+ and CD8+ T cells from the spleen did not change with ED administration of CD4 in either group (data not shown).

We next examined CD44 expression on CD4+ T

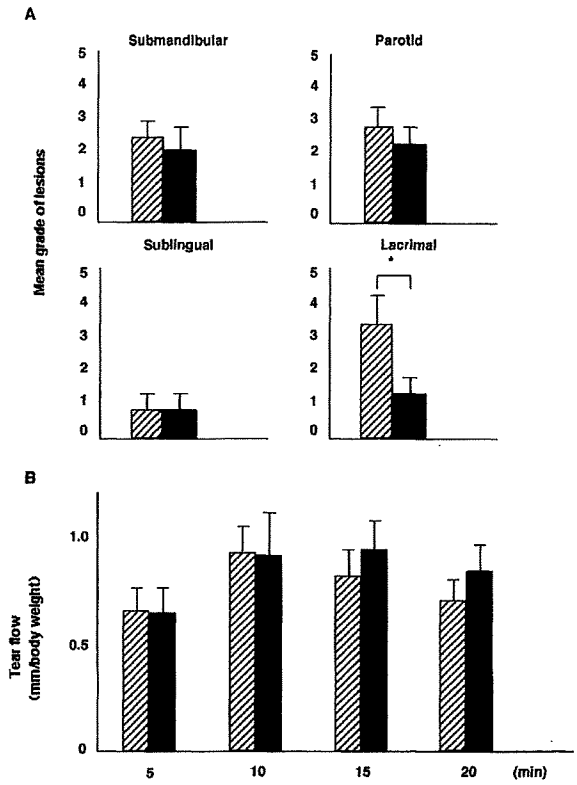

Figure 4. Prevention of the progression of autoimmune responses by ED administration of CD4 in lacrimal glands only. **A,** The 3d-Tx mice were treated with ED administration of control IgG (hatched bars) or anti-CD4 mAb (solid bars) from ages 10 to 12 weeks. The lacrimal, parotid, submandibular, or sublingual glands were removed 2 weeks after initial treatment and stained with hematoxylin and eosin. The histologic scores of each gland were evaluated as described in Materials and Methods. Values are the mean and SEM of 7 mice. * = $P < 0.05$. **B,** The 3d-Tx mice were treated with ED administration of control IgG (hatched bars) or anti-CD4 mAb (solid bars) from ages 10 to 12 weeks. The tear volume of each mouse was evaluated as described in Materials and Methods. Values are the mean and SEM of 5 mice. See Figure 2 for definitions.

cells because CD44 is known to be highly expressed on activated T cells and memory T cells (29). Lymph node CD4+ T cells from mice treated with ED administration of CD4 from ages 4 to 8 weeks and ages 10 to 12 weeks expressed lower levels of CD44 compared with those from the control IgG-treated group (Figures 5A and B). In contrast, the expression level of CD44 on splenic CD4+ T cells from 3d-Tx mice treated with ED administration of CD4 was similar to that from control IgG-treated mice (data not shown). Taken together, these results demonstrate that ED administration of CD4 inhibited the activation of CD4+ T cells infiltrating into the lacrimal glands, but did not delete the CD4+ T cells.

Reduction of JS-1–specific T cell response by ED administration of CD4. We previously reported that CD4+ T cells from 3d-Tx mice responded to the α-fodrin JS-1 peptide (13). Thus, we examined whether ED administration of CD4 affects the JS-1–specific proliferative response of lymph node cells from 3d-Tx mice. Cervical lymph node cells were purified after ED administration of CD4 from 4 to 8 weeks of age or 10 to 12 weeks of age and were stimulated with JS-1 or Con A. As previously reported, lymph node T cells from control IgG-treated mice at 8 to 12 weeks of age vigorously proliferated in response to JS-1 (Figures 6A and B). In contrast, the JS-1–specific T cell responses were lower in mice treated with ED administration of CD4 both from 4 to 8 weeks of age and 10 to 12 weeks of age than in

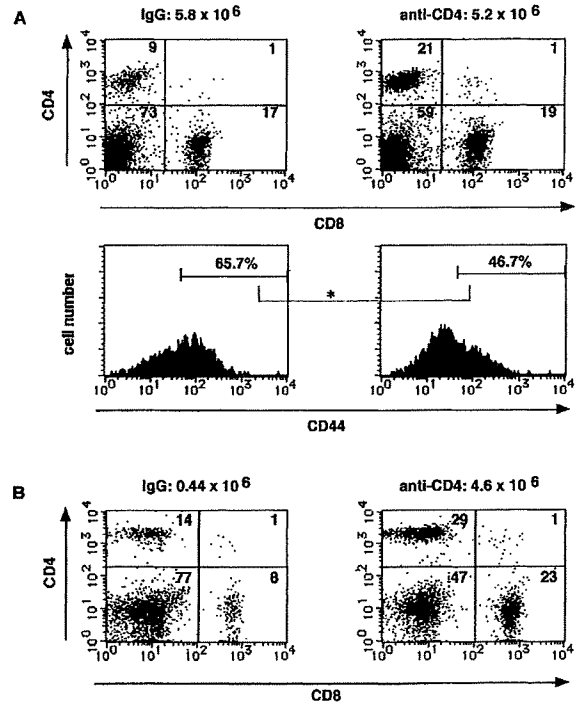

Figure 5. Flow cytometric analysis of lymph node cells. Cervical lymph node cells from 3d-Tx mice that were treated with ED administration of control IgG or anti-CD4 mAb from ages 4 to 8 weeks (**A**) or ages 10 to 12 weeks (**B**) were stained with phycoerythrin (PE)–conjugated anti-CD4 mAb and fluorescein isothiocyanate–conjugated anti-CD8 mAb or PE-conjugated anti-CD44 mAb and cytochrome-conjugated anti-CD44 mAb and analyzed by flow cytometry. The total cell number is indicated across the top. Results are representative of at least 3 independent experiments. * = $P < 0.05$ by Student's unpaired *t*-test. See Figure 2 for other definitions.

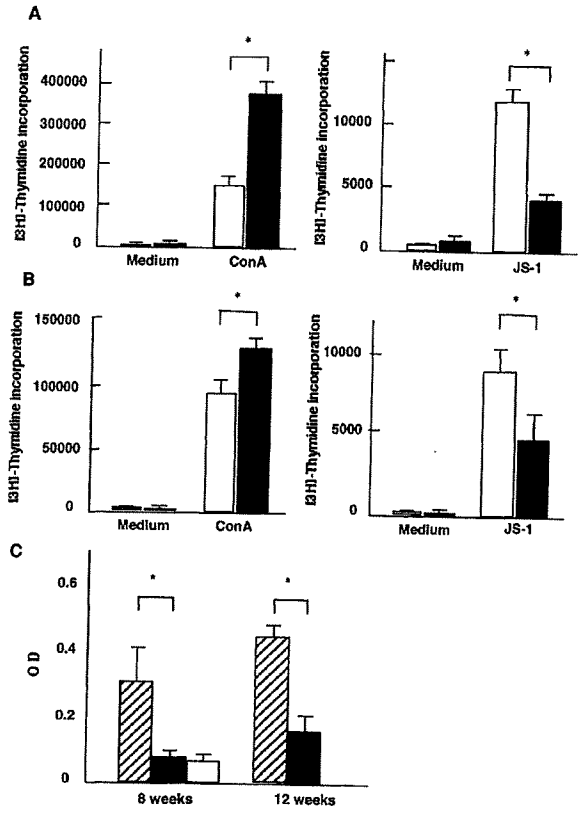

Figure 6. Proliferative response of JS-1–specific T cells and serum titer of anti–JS-1 antibody. The cervical lymph node cells from 3d-Tx mice that were treated with ED administration of control IgG **(left)** or anti-CD4 mAb **(right)** from **A,** ages 4 to 8 weeks or **B,** ages 10 to 12 weeks were stimulated with JS-1 peptide or concanavalin A (Con A) for 72 hours, and incorporation of ^{3}H-thymidine into cells during the final 12 hours was evaluated. Values are the mean and SEM of 7 mice. * = $P < 0.01$. **C,** Levels of serum autoantibody against 120-kd α-fodrin (JS-1) in 3d-Tx mice that were treated with ED administration of control IgG (hatched bars) or anti-CD4 mAb (solid bars) from ages 4 to 8 weeks or ages 10 to 12 weeks were measured by enzyme-linked immunosorbent assay. Non-Tx mice were used as controls (open bars). Values are the mean and SEM of 7 mice. OD = optical density; * = $P < 0.05$. See Figure 2 for other definitions.

control IgG-treated mice (Figures 6A and B). The inhibitory effects of anti-CD4 mAb appeared to be stronger when administered from 8 to 12 weeks of age (Figures 6A and B). The response to Con A was higher in groups treated with ED administration of CD4 (Figures 6A and B), arguing against the possibility that ED administration of CD4 suppressed total T cell responses. These results demonstrate the reduced expansion of JS-1–specific T cells in mice treated with ED administration of CD4, which is consistent with the low CD44 expression on CD4+ T cells from mice treated with ED administration of CD4.

Reduced titer of serum antibody against α-fodrin. The 3d-Tx mice have high titers of serum autoantibody against recombinant α-fodrin protein (JS-1) (12). Thus, we examined whether the local treatment with ED administration of CD4 affected serum levels of autoantibody against α-fodrin in the mice with SS. The titer of serum antibody against α-fodrin was evaluated after treatment of 3d-Tx mice with ED administration of CD4 from 4 to 8 weeks of age or 10 to 12 weeks of age. As shown in Figure 6, the titer of autoantibody against α-fodrin was lower in mice treated from ages 4 to 8 weeks and ages 10 to 12 weeks compared with control IgG-treated groups (Figure 6C). The decreased serum titer of autoantibody against α-fodrin suggests that ED administration of CD4 affected autoimmune pathology only in the lacrimal glands but was able to suppress systemic production of α-fodrin–specific autoantibody.

DISCUSSION

Patients with SS have generally been treated with systemic administration of immunosuppressive drugs (10,21). Despite the effectiveness of such drugs, it is better to establish a local therapeutic strategy for eye and mouth symptoms of SS because the systemic use of immunosuppressive drugs induces severe side effects (21). In this study, we evaluated whether ED administration of CD4 effectively inhibits autoimmune pathology in the lacrimal glands of a mouse model of SS (12). We have previously reported that anti-CD86 mAb treatment improved the autoimmune pathology in both the lacrimal and the salivary glands of mice with SS (30). We used an antibody because the specific binding ability of a mAb against the target molecule allows the establishment of a molecule-specific therapeutic strategy with fewer side effects. Although an antibody is a large molecular weight glycoprotein, we demonstrated that ED administration of CD4 effectively inhibited both the onset and the progression of autoimmune responses only in the lacrimal glands of mice with SS. Although we did not simply compare the efficacy of topical administration of anti-CD4 mAb with that of systemic administration, this successful therapeutic effect of anti-CD4 mAb would provide the possibility of establishing a new form of antibody-based therapy for patients with eye symptoms caused by SS as well as other types of diseases.

ED administration of CD4 increased the total number of CD4+ T cells in cervical lymph nodes after a

4-week treatment starting at the age of 4 weeks, and increased both CD4+ and CD8+ T cells after a 2-week treatment starting at the age of 10 weeks. After ED administration of CD4, the resultant CD4+ T cells expressed low levels of CD44 compared with those after treatment with control IgG. The results suggest that the main therapeutic effect of the anti-CD4 mAb in the pathology of SS is the inhbition of CD4+ T cell activation rather than the deletion of CD4+ T cells, although the anti-CD4 mAb both blocks the interaction between CD4 and class II MHC and deletes CD4+ T cells in vivo (27,28). The increase in T cells after ED administration of CD4 would be due to reduced CD4+ T cell activation, resulting in a decrease in the activation-induced death of CD4+ T cells, which may explain the larger relative cell numbers in the anti-CD4 mAb–treated mice than in the control IgG-treated mice. This is supported by results from a previous study (20) demonstrating increased CD4+ T cell apoptosis in humans with SS. Furthermore, in our preliminary experiments, we observed a decrease in annexin V–positive CD4+ T cells in lymph nodes from mice treated with ED administration of CD4 (data not shown).

Nevertheless, it will be important to evaluate the mechanistic basis of the effect of anti-CD4 mAb. In particular, the number of lymphocytes in the lacrimal glands significantly decreased after a 2-week treatment of ED administration of CD4 starting at 10 weeks of age, which suggests the contribution of cytolytic as well as inhibitory activity of anti-CD4 mAb to the inhibition of autoimmune pathology. In addition, the suppressed activation of CD4+ T cells might decrease the activation of antigen-presenting cells or direct the help of CD8+ T cells, which also suppresses the initial expansion of CD8+ T cells, resulting in activation-induced cell death from ages 10 to 12 weeks but not ages 4 to 8 weeks. The differential mode of activation of CD8+ T cells during the initial and progression stages of diseases suggests that CD8+ T cells are required in the progression stage of SS. We are currently performing experiments using anti-CD8 mAb eyedrops to address this issue.

One might argue whether CD25+ regulatory T cells play some role in the effect of ED administration of CD4 in this mouse model because a thymectomy was performed 3 days after birth in the mice with SS. However, we do not think that CD25+ regulatory T cells significantly contribute to the therapeutic effect of ED administration of CD4 because the relative number of CD25+ T cells in regional lymph nodes is not increased in mice treated with ED administration of CD4 (data not shown). Recently, several groups have demonstrated that regulatory T cells differentiated from naive CD25+ T cells (31,32), although there are no appropriate cell surface markers to distinguish such regulatory T cells from effector T cells. Thus, it would be interesting to evaluate the contribution of such regulatory T cells to the inhibition of autoimmune pathology by ED administration of CD4.

ED administration of CD4 inhibited CD4+ T cell activation in cervical lymph node cells but not spleen cells, indicating that anti-CD4 mAb locally affects T cell activation. Although an antibody is a high molecular weight glycoprotein, we have observed the localization of anti-CD4 mAb in the lacrimal glands but not the spleen or regional lymph nodes (Hayashi Y, et al: unpublished observations). Thus, we think that anti-CD4 mAb blocks the activation of pathologic CD4+ T cells by interfering with class II MHC interactions in the lacrimal glands. Nevertheless, it remains unclear how large glycoproteins migrate into the parenchyma of the lacrimal glands, and this must be addressed in a future study.

We showed that ED administration of CD4 reduces serum anti–JS-1 autoantibody levels. These results suggest that ED administration of CD4 inhibited local JS-1–specific CD4+ T cell activation, which impaired T cell help to activate JS-1–specific B cells. Although ED administration of CD4 inhibited autoimmune pathology only in the lacrimal glands, it almost completely eliminated serum JS-1–specific autoantibody. There are 2 possible explanations for this result. The first is that the major helper T cells to induce JS-1–specific autoantibody might be from infiltrating T cells in the lacrimal glands. However, we think this possibility is unlikely because α-fodrin protein is present both in the lacrimal and the salivary glands, and transfer of infiltrating CD4+ T cells into the salivary glands in normal mice is able to cause SS-like lesions with autoantibody production (33). The second possibility is that ED administration of CD4 can prevent T cell help to activate B cells both in the lacrimal and the salivary glands but cannot sufficiently suppress autoimmune pathology in the salivary glands. The direct contribution of CD4+ T cells in the absence of B cells to the autoimmune pathology in this mouse model should be evaluated to address this possibility.

Several groups have examined the effect of ED administration of CSA as a treatment for SS and reported on its positive effect on autoimmune pathology (22,34). However, since systemic injection of CSA induces severe side effects in renal arteries (10), it is possible that even CSA eyedrops can induce some side effects in the eye. In this regard, antibodies have the ability to bind very specifically to their target receptor,

which suggests that it is possible to establish a therapeutic strategy with fewer side effects. Indeed, the application of 2 μg of anti-CD4 mAb daily did not induce any side effects histologically (data not shown). We did not observe any changes in cell number or activation status in the spleen with ED administration of CD4, which repudiates the possibility that anti-CD4 mAb enters into the circulation.

Several aspects of this model system illustrate important issues for future trials with antibody-based therapeutics. A variety of cell surface molecules have been reported to be responsible for the progression of eye symptoms in SS as well as other diseases (17,35,36). Thus, this antibody-based topical therapy may also be applicable to other types of antibodies or diseases.

REFERENCES

1. Sebzda E, Mariathasan S, Ohteki T, Jones R, Bachmann MF, Ohashi PS. Selection of the T cell repertoire. Annu Rev Immunol 1999;17:829–74.
2. Starr TK, Jameson SC, Hogquist KA. Positive and negative selection of T cells. Annu Rev Immunol 2003;21:139–76.
3. Schwartz RH. T cell anergy. Annu Rev Immunol 2003;21:305–34.
4. Lenardo M, Chan KM, Hornung F, McFarland H, Siegel R, Wang J, et al. Mature T lymphocyte apoptosis—immune regulation in a dynamic and unpredictable antigenic environment. Annu Rev Immunol 1999;17:221–53.
5. Wakeland EK, Liu K, Graham RR, Behrens TW. Delineating the genetic basis of systemic lupus erythematosus. Immunity 2001;15: 397–408.
6. Yasutomo K. Pathological lymphocyte activation by defective clearance of self-ligands in systemic lupus erythematosus. Rheumatology (Oxford) 2003;42:214–22.
7. Marrack P, Kappler J, Kotzin BL. Autoimmune disease: why and where it occurs. Nat Med 2001;7:899–905.
8. Davidson A, Diamond B. Autoimmune diseases. N Engl J Med 2001;345:340–50.
9. Yasutomo K, Horiuchi T, Kagami S, Tsukamoto H, Hashimura C, Urushihara M, et al. Mutation of DNASE1 in people with systemic lupus erythematosus. Nat Genet 2001;28:313–4.
10. Fox RI, Stern M, Michelson P. Update in Sjogren syndrome. Curr Opin Rheumatol 2000;12:391–8.
11. Gordon TP, Bolstad AI, Rischmueller M, Jonsson R, Waterman SA. Autoantibodies in primary Sjogren's syndrome: new insights into mechanisms of autoantibody diversification and disease pathogenesis. Autoimmunity 2001;34:123–32.
12. Haneji N, Nakamura T, Takio K, Yanagi K, Higashiyama H, Saito I, et al. Identification of α-fodrin as a candidate autoantigen in primary Sjogren's syndrome. Science 1997;276:604–7.
13. Saegusa K, Ishimaru N, Yanagi K, Arakaki R, Ogawa K, Saito I, et al. Cathepsin S inhibitor prevents autoantigen presentation and autoimmunity. J Clin Invest 2002;110:361–9.
14. Saegusa K, Ishimaru N, Yanagi K, Mishima K, Arakaki R, Suda T, et al. Prevention and induction of autoimmune exocrinopathy is dependent on pathogenic autoantigen cleavage in murine Sjogren's syndrome. J Immunol 2002;169:1050–7.
15. Watanabe T, Tsuchida T, Kanda N, Mori K, Hayashi Y, Tamaki K. Anti-α-fodrin antibodies in Sjogren syndrome and lupus erythematosus. Arch Dermatol 1999;135:535–9.
16. Ohno K, Takahashi T, Maki K, Ueda M, Taguchi O. Successful transfer of localized autoimmunity with positively selected CD4+ cells to scid mice lacking functional B cells. Autoimmunity 1999; 29:103–10.
17. Tabbara K, Sharara N. Sjogren's syndrome: pathogenesis. Eur J Ophthalmol 1999;9:1–7.
18. Hayashi Y, Haneji N, Hamano H. Pathogenesis of Sjogren's syndrome-like autoimmune lesions in MRL/lpr mice. Pathol Int 1994;44:559–68.
19. Kohriyama K, Katayama Y. Disproportion of helper T cell subsets in peripheral blood of patients with primary Sjogren's syndrome. Autoimmunity 2000;32:67–72.
20. Zeher M, Szodoray P, Gyimesi E, Szondy Z. Correlation of increased susceptibility to apoptosis of CD4+ T cells with lymphocyte activation and activity of disease in patients with primary Sjogren's syndrome. Arthritis Rheum 1999;42:1673–81.
21. Fox RI, Maruyama T. Pathogenesis and treatment of Sjogren's syndrome. Curr Opin Rheumatol 1997;9:393–9.
22. Kunert KS, Tisdale AS, Stern ME, Smith JA, Gipson IK. Analysis of topical cyclosporine treatment of patients with dry eye syndrome: effect on conjunctival lymphocytes. Arch Ophthalmol 2000;118:1489–96.
23. Hayashi Y, Kojima A, Hata M, Hirokawa K. A new mutation involving the sublingual gland in NFS/N mice: partially arrested mucous cell differentiation. Am J Pathol 1988;132:187–91.
24. Haneji N, Hamano H, Yanagi K, Hayashi Y. A new animal model for primary Sjogren's syndrome in NFS/sld mutant mice. J Immunol 1994;153:2769–77.
25. White SC, Casarett GW. Induction of experimental autoallergic sialadenitis. J Immunol 1974;112:178–85.
26. Delporte C, O'Connell BC, He X, Lancaster HE, O'Connell AC, Agre P, et al. Increased fluid secretion after adenoviral-mediated transfer of the aquaporin-1 cDNA to irradiated rat salivary glands. Proc Natl Acad Sci U S A 1997;94:3268–73.
27. Ghobrial RR, Boublik M, Winn HJ, Auchincloss H Jr. In vivo use of monoclonal antibodies against murine T cell antigens. Clin Immunol Immunopathol 1989;52:486–506.
28. Madrenas J, Chau LA, Smith J, Bluestone JA, Germain RN. The efficiency of CD4 recruitment to ligand-engaged TCR controls the agonist/partial agonist properties of peptide-MHC molecule ligands. J Exp Med 1997;185:219–29.
29. Anderson BE, McNiff J, Yan J, Doyle H, Mamula M, Shlomchik MJ, et al. Memory CD4+ T cells do not induce graft-versus-host disease. J Clin Invest 2003;112:101–8.
30. Saegusa K, Ishimaru N, Yanagi K, Haneji N, Nishino M, Azuma M, et al. Treatment with anti-CD86 costimulatory molecule prevents the autoimmune lesions in murine Sjogren's syndrome (SS) through up-regulated Th2 response. Clin Exp Immunol 2000;119: 354–60.
31. Sakaguchi S. Naturally arising CD4+ regulatory T cells for immunologic self-tolerance and negative control of immune responses. Annu Rev Immunol 2004;22:531–62.
32. Jonuleit H, Schmitt E. The regulatory T cell family: distinct subsets and their interrelations. J Immunol 2003;171:6323–7.
33. Hayashi Y, Haneji N, Hamano H, Yanagi K. Transfer of Sjogren's syndrome-like autoimmune lesions into SCID mice and prevention of lesions by anti-CD4 and anti-T cell receptor antibody treatment. Eur J Immunol 1994;24:2826–31.
34. Tsubota K, Saito I, Ishimaru N, Hayashi Y. Use of topical cyclosporin A in a primary Sjogren's syndrome mouse model. Invest Ophthalmol Vis Sci 1998;39:1551–9.
35. Tornwall J, Lane TE, Fox RI, Fox HS. T cell attractant chemokine expression initiates lacrimal gland destruction in nonobese diabetic mice. Lab Invest 1999;79:1719–26.
36. Amft N, Bowman SJ. Chemokines and cell trafficking in Sjogren's syndrome. Scand J Immunol 2001;54:62–9.

0013-7227/04/$15.00/0
Printed in U.S.A.

Endocrinology 145(5):2384–2391
Copyright © 2004 by The Endocrine Society
doi: 10.1210/en.2003-1536

Estrogen Deficiency Accelerates Murine Autoimmune Arthritis Associated with Receptor Activator of Nuclear Factor-κB Ligand-Mediated Osteoclastogenesis

TOMOKO YONEDA, NAOZUMI ISHIMARU, RIEKO ARAKAKI, MASARU KOBAYASHI, TAKASHI IZAWA, KEIJI MORIYAMA, AND YOSHIO HAYASHI

Departments of Pathology (T.Y., N.I., R.A., M.K., T.I., Y.H.) and Orthodontics (T.Y., T.I., K.M.), Tokushima University School of Dentistry, Tokushima 770-8504 Japan

The aims of this study were to evaluate the *in vivo* effects of estrogen deficiency in MRL/*lpr* mice as a model for rheumatoid arthritis and to analyze the possible relationship between immune dysregulation and receptor activator of nuclear factor-κB ligand (RANKL)-mediated osteoclastogenesis. Experimental studies were performed in ovariectomized (Ovx)-MRL/*lpr*, Ovx-MRL+/+, sham-operated-MRL/*lpr*, and sham-operated-MRL+/+ mice. Severe autoimmune arthritis developed in younger Ovx-MRL/*lpr* mice until 24 wk of age, whereas these lesions were entirely recovered by pharmacological levels of estrogen administration. A significant elevation in serum rheumatoid factor, anti-double-stranded DNA, and anti-type II collagen was found in Ovx-MRL/*lpr* mice and recovered in mice that underwent estrogen administration. A high proportion of $CD4^+$ T cells bearing RANKL was found, and an enhanced expression of RANKL mRNA and an impaired osteoprotegerin mRNA was detected in the synovium. An increase in both osteoclast formation and bone resorption pits was found. These results indicate that estrogen deficiency may play a crucial role in acceleration of autoimmune arthritis associated with RANKL-mediated osteoclastogenesis in a murine model for rheumatoid arthritis. (*Endocrinology* 145: 2384–2391, 2004)

IT IS WELL KNOWN that sex steroids have significant impact on the development of autoimmune diseases in both humans and rodents. In particular, estrogen has been suggested to be responsible for the strong female preponderance of the human rheumatoid arthritis (RA), systemic lupus erythematosus, scleroderma, and Sjögren's syndrome (1–3), but the role of estrogens in the female has not been fully characterized. RA is a chronic inflammatory disease characterized by invasive synovial hyperplasia leading to progressive joint destruction. Rheumatoid synovial cells are not only morphologically characterized by their transformed appearance (4) but also are phenotypically transformed to proliferate abnormally (5, 6). These cells invade bone and cartilage by producing an elevated amount of proinflammatory cytokines (7) and matrix metalloproteinases (MMPs) (8) and by inducing osteoclast (OC) formation and activation (9, 10).

OCs, the multinucleated cells exclusively responsible for bone resorption, have been observed to resorb bone actively at the site of invasion of the proliferated synovial membrane into the adjacent bone (11). The cell types responsible for bone resorption in RA have been characterized as authentic OCs (12), and it was reported that rheumatoid synovial fibroblasts are involved in bone destruction by inducing osteoclastogenesis (13). However, the exact mechanisms involved in the formation and activation of OCs in RA are still unclear.

Receptor activator of nuclear facto-κB ligand (RANKL) (14) is a regulator of the immune system and of bone development (15). RANKL is expressed on activated T cells (16), and a major target for RANKL in the immune system appears to be mature dendritic cells (DCs) that express a high level of RANKL receptor (RANK) (17). *In vitro*, RANKL promotes the survival of mature DCs, most likely by up-regulating the expression of Bcl-XL (18), and induces the production of proinflammatory cytokines, such as IL-1 and IL-6, and cytokines that stimulate and induce differentiation of T cells, such as IL-12 and IL-15 (19). Therefore, RANKL is likely to act as a positive-feedback regulator during productive T cell-DC interactions (20).

The MRL/*lpr* mouse strain was chosen to test the estrogenic action because it has a genetic predisposition to arthritis with characteristics similar to those of human RA including cell infiltration, pannus formation, bone and cartilage breakdown, and the presence of serum rheumatoid factor (RF) (21–23). The aim of this study was to analyze the *in vivo* effects of estrogen deficiency on the development of autoimmune arthritis in MRL/*lpr* mice and to evaluate the possible relationship with RANKL-mediated osteoclastogenesis.

Abbreviations: Ab, Antibody; CII, type 2 collagen; DC, dendritic cell; dsDNA, double-stranded DNA; ER, estrogen receptor; IFN, interferon; IRF, IFN regulatory factor; LN, lymph node; mAb, monoclonal antibody; MMP, matrix metalloproteinase; OC, osteoclast; OPG, osteoprotegerin; Ovx, ovariectomized; RA, rheumatoid arthritis; RANK, RANKL receptor; RANKL, receptor activator of nuclear factor-κB ligand; RF, rheumatoid factor; sham, sham-operated; TRAP, tartrate-resistant acid phosphatase.

Endocrinology is published monthly by The Endocrine Society (http://www.endo-society.org), the foremost professional society serving the endocrine community.

Materials and Methods

Mice and treatment

MRL/Mp-*lpr*/*lpr* (MRL/*lpr*, age 4–24 wk; n = 108) and MRL+/+ mice (age 4–24 wk; n = 58) were purchased from Charles River Japan

Inc. (Atsugi, Japan), and were fed under specific pathogen-free conditions. Female MRL/*lpr* mice and MRL+/+ mice (4 wk of age) were ovariectomized (Ovx) and compared with sham-operated (sham)-MRL/*lpr* and MRL+/+ mice. Six to 10 mice in each group were analyzed at 8, 12, 16, 20, and 24 wk of age. Ovx-MRL/*lpr* mice were administered im with 60 mg/kg·wk estrogen (Ovahormine depo; Teikoku Zouki Inc., Tokyo, Japan) in sesame oil or sc with 25 mg/kg·d testosterone (Wako Pure Chemical, Osaka, Japan) from 4–20 wk of age. Care of the mice was in accordance with institutional guidelines.

Histology and immunohistology

All organs were removed from the mice and fixed with 10% phosphate-buffered formalin, and ankles were further decalcified in 10% EDTA. Sections (4 μm in thickness) were stained with hematoxylin and eosin. Histological grading of inflammatory arthritis was done according to the methods by Edwards *et al.* (24) as follows: one point score indicates hyperplasia/hypertrophy of synovial cells; fibrosis/fibroplasia; proliferation of cartilage and bone; destruction of cartilage and bone; and/or mononuclear cell infiltrate. Immunohistological analysis was performed on freshly frozen sections (4 μm in thickness) by the biotin-avidin immunoperoxidase method using ABC reagent (Vector Laboratories Inc., Burlingame, CA). The monoclonal antibodies (mAb) used were biotinylated rat mAbs to CD4, CD8 (BD Biosciences, San Jose, CA), and mouse RANKL (IMGENEX, San Diego, CA).

Flow cytometric analysis

Spleen and inguinal lymph node (LN) cell suspensions were stained with antibodies (Ab) conjugated to phycoerythrin (anti-CD4, Cedarlane Laboratories Ltd., Ontario, Canada; B220, PharMingen, San Diego, CA), fluorescein isothiocyanate (anti-CD8, Cedarlane Laboratories; Thy1.2, PharMingen), and antimouse RANKL (IMGENEX) and analyzed with EPICS (Coulter, Miami, FL).

Measurement of anti-double-stranded DNA (dsDNA) Ab, RF, and type 2 collagen (CII) Ab levels

Anti-dsDNA Abs, RF, and anti-CII Ab were detected by ELISA as described previously (25–27). Briefly, flat-bottom plates (Nalge Nunc International, Roskilde, Denmark) were coated with 1.5 μg/ml of native calf thymus DNA (Life Technologies, Inc., Rockville, MD) in buffer containing 0.1 M sodium bicarbonate and 0.05 M citric acid at 4 C overnight. Serum samples were serially diluted (starting at 1/200) and added to the plates for a 1-h incubation at 37 C. After washing, peroxidase-conjugated goat antimouse IgG, or IgM (Southern Biotechnology Associates, Birmingham, AL), was added and incubated for 1 h at 37 C. Ab binding was visualized using orthophenylenediamine (Sigma, St. Louis, MO). For the measurement of IgG and IgM RF, human IgG and IgM (Chemicon International, Temecula, CA) were coated onto plates at 10 μg/ml in carbonate buffer, and the same procedures were followed as described above. For the measurement of serum Abs to CII, native bovine CII was dissolved in 0.1 M acetic acid at 1 mg/ml and diluted with 0.1 M sodium bicarbonate at 10 μg/ml (pH 9.6). The microtiter plate was coated with 100 μl of CII antigen solution. After washing three times, 100 μl per well of serum samples that had been serially diluted in PBS/Tween 20/1% BSA and control serum were added and incubated for 1 h at 37 C. After washing, peroxidase-conjugated goat antimouse IgG (at 1.4 μg/ml, 100 μl per well) (Organon Teknika, Durham, NC) was added and incubated for 1 h at 37 C. A total of 100 μl o-phenylenediamine (0.5 mg/ml) dissolved in 0.1 M citrate buffer (pH 5.0) containing 0.012% H_2O_2 was added, and the reaction was stopped using 8 N H_2SO_4 (20 μl per well).

Measurement of cytokine production

Cytokine production was tested by two-step sandwich ELISA using a mouse IL-2, IL-4, and interferon (IFN)-γ kit (Genzyme, Cambridge, MA). In brief, culture supernatants from LN cells activated with immobilized anti-CD3 mAb (Cedarlane Laboratories) for 3 d were added to microtiter plates precoated with anti-IL-2, IL-4, and IFN-γ capture Ab and incubated overnight at 4 C. After addition of biotinylated detecting Ab and incubation at room temperature for 45 min, avidin-peroxidase was added and incubated at room temperature for 30 min. Finally, 2,2′-azino-di-3-ethylbenzthiazoline sulfonate substrate containing H_2O_2 was added, and the colorimetric reaction was read at an absorbance of 405 nm using an automatic microplate reader (Bio-Rad Laboratories Inc., Hercules, CA). The concentrations of IL-2 (picograms per milliliter), IL-4 (picograms per milliliter), and IFN-γ (picograms per milliliter) were calculated according to the standard curves produced by various concentrations of recombinant cytokines.

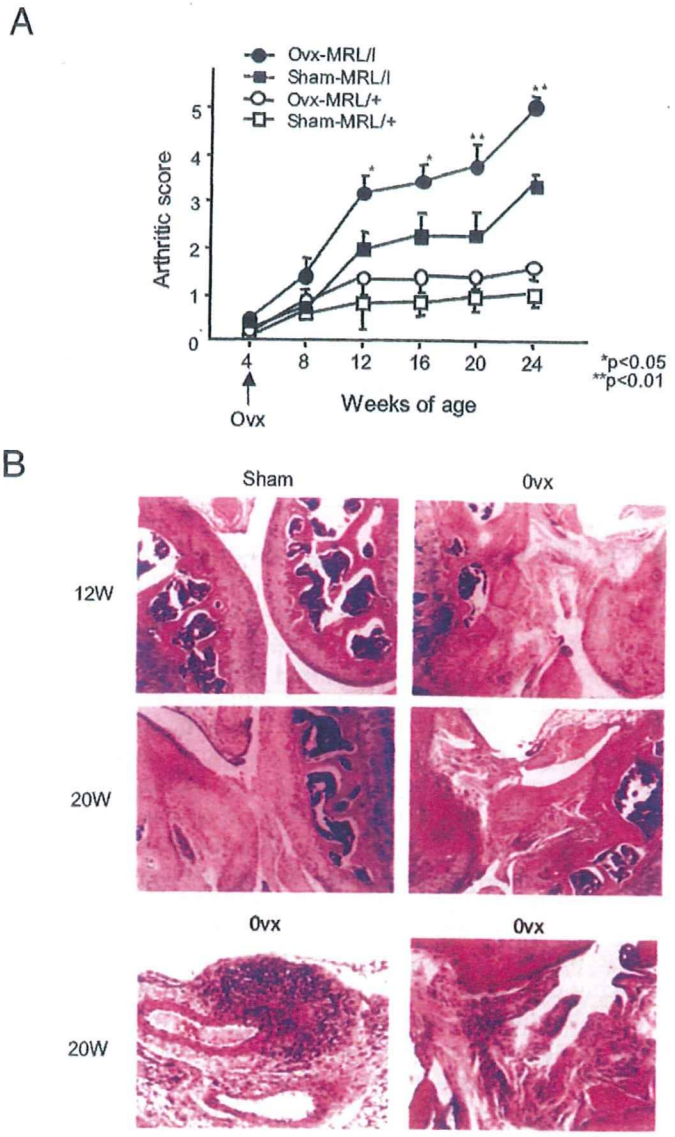

FIG. 1. Effects of the Ovx on joint histopathology. Histological score of autoimmune arthropathy developed in younger Ovx-MRL/*lpr* mice compared with those in sham-MRL/*lpr* and Ovx-MRL+/+ mice until 24 wk of age (A). Histological evaluation of the knee joints was performed according to the methods by Edwards *et al.* (24) (*, $P < 0.05$; and **, $P < 0.01$, Student's *t* test). Representative photomicrographs taken from Ovx- and sham-MRL/*lpr* mice at 12 (12W) and 20 wk (20W) of age (B). The histopathological effects observed in Ovx-MRL/*lpr* mice at age 20 wk included mononuclear cell infiltration into the subsynovial tissue (*lower left*), and synovial hyperplasia (*lower right*) (hematoxylin and eosin). In contrast, mononuclear cell infiltration and bone and cartilage pathology was absent in sham-MRL/*lpr* mice until 20 wk of age (*middle left*).

ELISA for murine osteoprotegerin (OPG)

An anti-murine OPG mAb (TECHNE Corp., Minneapolis, MN) was diluted with 0.1 M sodium bicarbonate (pH 9.6) solution to a concentration of 10 μg/ml, and the 100-μl aliquot was added to each well of 96-well plates. After incubation at 4 C overnight, the capture solution was removed by flicking the plates, and the wells were blocked with the blocking solution (300 μl per well) for 2 h at room temperature. Recombinant OPG (100 μl) (R&D System Inc., Minneapolis, MN) standard and a series of test samples were added to the wells, and the plates were incubated for 2 h at room temperature. The wells were then washed with the washing buffer, and 100 μl of peroxidase-labeled anti-OPG mAb was added to each well. After incubation for an additional 2 h, 100 μl of tetramethylbenzidine substrate reagent was added to each well. Tetramethylbenzidine stop buffer (100 μl) was added to each well, and absorbance at 450 nm of the wells was measured with a microplate reader (Bio-Rad Laboratories Inc.).

RT-PCR

The total RNA from LNs and synovial tissues was extracted as reported previously (28). The RNA was reverse-transcribed into cDNA. The cDNA reaction mixture was diluted with 90 μl of PCR buffer and mixed with 500 nM of the 5′ and 3′ primers, 0.1 mM deoxynucleotide triphosphate mix, 2 mM $MgCl_2$, and 2 U thermostable *Taq* polymerase (PerkinElmer Cetus, Norwalk, CT). The cDNA was subjected to enzymatic amplification in a DNA thermal cycler (PerkinElmer Cetus) by using specific primers. PCR was carried out at 55 C annealing temperature for 30–35 cycles. The specific primers used were as follows: IL-1β, TGA TGA GAA TGA CCT GTT CT and CTT CTT CAA AGA TGA AGG AAA; TNF-α, ATG AGC ACA GAA AGC ATG ATC and AGA TGA TCT GAG TGT GAG GG; IL-6, CTC TGC AAG AGA GAC TTC CAT and ATA GGC AAA TTT CCT GAT TAT A; IFN-γ, CCT CAG ACT CTT TGA ACT CT and CAG CGA CTC CTT TTC CGC TT; IFN regulatory factor (IRF)-1, TCT GAG TGG CAT ATG CAG ATG GAC and GGT CAG AGA CCC AAA CTA TGG TCG; MMP-1, ATG GTG GGG ATG CCC ATT TT and CAG CAT CTA CTT TGT TGC C; MMP-2, GAG TTG GCA GTG CAA TAC CT and GCC ATC CTT CTC AAA GTT GT; MMP-3, GAA ATG CAG AAG TTC CTC GG and GAG TTC CAT AGA GGG ACT GA; MMP-9, CCA TGA GTC CCT GGC AG and AGT ATG TGA TGT TAT GAT G; TIMP (tissue inhibitor of metalloproteinase)-1, CTG GCA TCC TCT TGT TGC TA and AGG GAT CTC CAA GTG CAC AA; RANKL, GGG AAT TAC AAA GTG CAC CAG and GCC ATC CTT CTC AAA GTT GT; RANK, GTC TTC TGG AAC CAT CTT CTC C and CAC AGA CAA ATG CAA ACC TTG; OPG, TCA AGT GCT TGA GGG CAT AC and TGG AGA TCG AAT TCT GCT TG; estrogen receptor (ER)-α, AAT TCT GAC AAT CGA CGC CAG and GTG CTT CAA CAT TCT CCC TCC TC; ER-β, TTC CCA GCA GCA CCG GTA ACC T and TCC CTC TTG GCG CTT GGA CTA; β-actin, GTG GGC CGC TCT AGG CAC CA and CGG TTG GCC TTA GGG TTC AGG GGG. The amplified DNA reaction mixture was subjected to 1.7% agarose gel electrophoresis, and the amplified product was visualized by UV fluorescence after staining with ethidium bromide.

Tartrate-resistant acid phosphatase (TRAP) staining

Staining for TRAP was performed according to the modified method of Takahashi *et al.* (29). Sections were rinsed once with PBS (pH 7.4), air dried, fixed with 10% formalin in PBS (pH 5.4) for 5 min, and fixed with

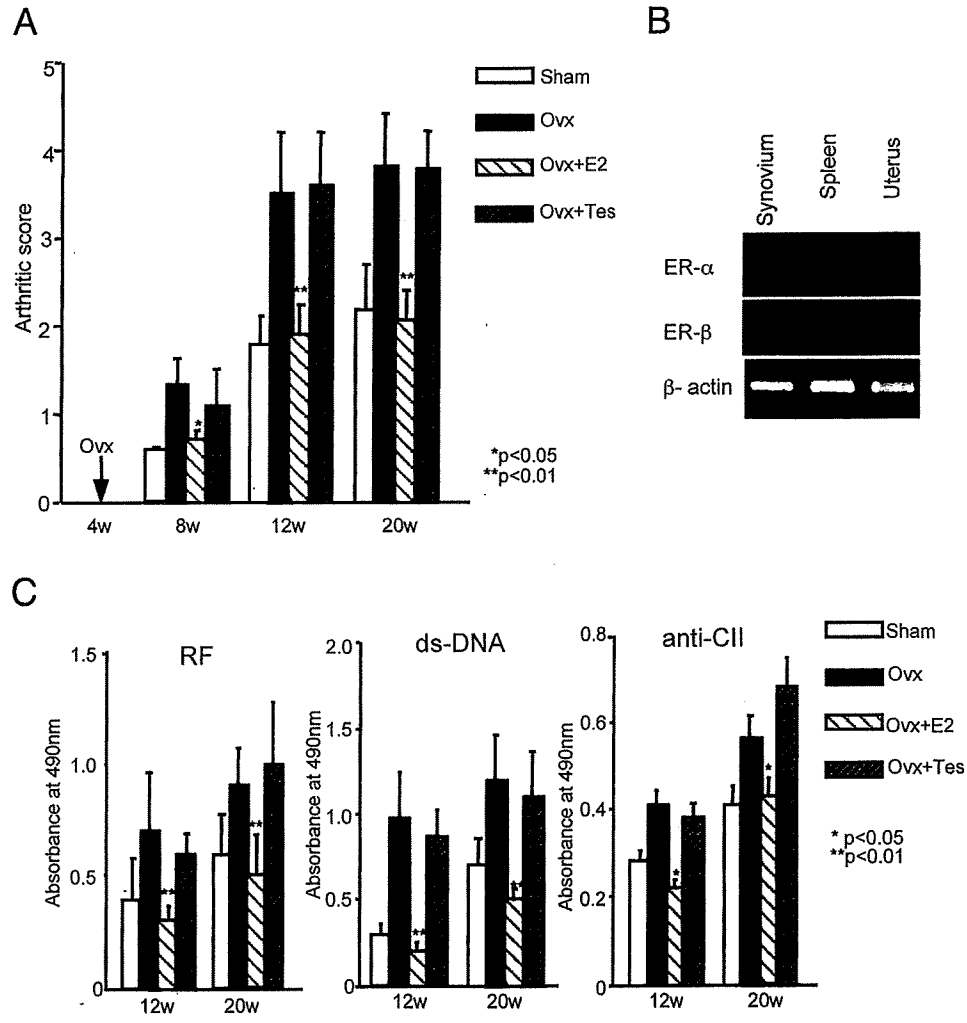

FIG. 2. The destructive lesions in the knee joints in Ovx-MRL/*lpr* mice were inhibited by estrogen administration (10^{-9} M) at ages 12 and 20 wk (*, $P < 0.05$ and **, $P < 0.01$, Student's *t* test) (A). Detection of gene expression in ER-α in the synovium but not in ER-β by RT-PCR analysis (B). E2, 17β-Estradiol. Serum RF, anti-dsDNA Abs, and anti-CII were significantly increased in Ovx-MRL/*lpr* mice compared with those in sham-MRL/*lpr* mice, and these changes were entirely recovered by the treatment with estrogen administration (10^{-9} M) at 12 and 20 wk of age (*, $P < 0.05$; and **, $P < 0.01$, Student's *t* test) (C). Tes, Testosterone.

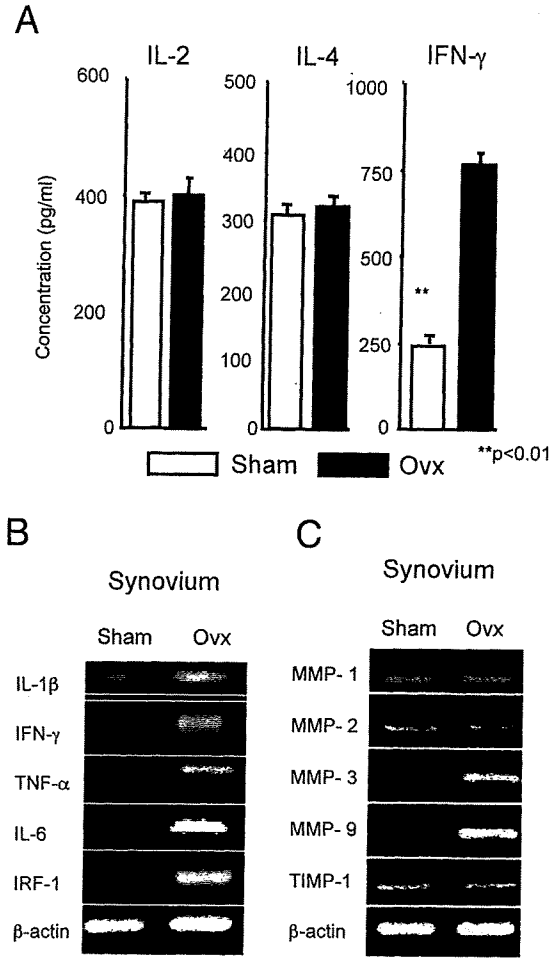

FIG. 3. Effects of the Ovx on expression of cytokines and MMPs. Culture supernatants from anti-CD3 mAb-stimulated LN T cells obtained from Ovx-MRL/*lpr* mice at age 20 wk contained high levels of IFN-γ (**, $P < 0.01$, Student's t test), whereas no different levels of IL-2 and IL-4 was observed by ELISA (A). Increased expressions of cytokine genes including IL-1β, IFN-γ, TNF-α, IL-6, IRF-1, and β-actin were detected in synovium from Ovx-MRL/*lpr* mice at age 20 wk, compared with those from sham-mice by RT-PCR analysis (B). Enhanced gene expressions of MMP-3, and MMP-9 mRNA were found in synovium from Ovx-MRL/*lpr* mice at age 20 wk (C).

methanol-acetone (50:50; pH 5.4) for 30 sec. The coverslips were air-dried and stained for 15 min at room temperature in a 0.1 M sodium acetate buffer (pH 5.0) containing naphthol AS-MX phosphate (Sigma) as a substrate and fast red violet LB salt (Sigma) as a stain for the reaction product in the presence of 50 mM of sodium tartrate.

Assessment of bone resorption

Bone marrow cells (5×10^5) from Ovx- and sham-MRL/*lpr* mice were added to the wells of 96-well plates containing a slice of bovine cortical bone and incubated in a total volume of 200 μl α-MEM-fetal bovine serum as described previously (30). All cultures were maintained in the presence of dexamethazone (10^{-7} M, FUNAKOSHI Pharmcol., Tokyo, Japan) and 1α,25-$(OH)_2D_3$ (10^{-8} M, Chugai Inc., Tokyo, Japan) for 10 d. Bone slices were assessed for bone resorptive activity, brushed with a rubber policeman to remove cells after observation under a microscope, and stained with Mayer's hematoxylin. Bone resorption pits were quantified by densitometric analysis of images of the whole area of bone slices as previously described (30). Additionally, *in vitro* osteoclastogenesis was assayed using bone marrow-derived TRAP-positive cells with macrophage colony stimulating factor (5 ng/ml; PeproTech EC, London, UK), recombinant murine RANKL (10 ng/ml; PeproTech Inc., Rocky Hill, NJ), recombinant OPG (100 ng/ml; R&D Systems Inc.), and 17β-estradiol (10^{-9} M), at indicated concentration after the estimation of dose responses.

Results

Effects of the Ovx on joint histopathology

Destructive autoimmune arthritis developed in young Ovx-MRL/*lpr* mice, not in young sham-MRL/*lpr* and Ovx-MRL+/+ mice, and these lesions aggravated with age from 12 until 24 wk of age. Histological analysis of the knee joints was performed at 8, 12, 16, 20, and 24 wk of age for all the experiments. Analysis of the histological results for the experiment, shown in Fig. 1A, indicates that the group that was treated with Ovx had significant higher subsynovial inflammation, synovial hyperplasia, pannus formation and cartilage erosion, bone destruction, and overall histopathology. Shown in Fig. 1B are photomicrographs taken from representative Ovx- and sham-MRL/*lpr* mice at 12 and 20 wk of age. The effects observed in Ovx-MRL/*lpr* mice included synovial hyperplasia, pannus formation, bone erosion, and infiltration of mononuclear cells into the subsynovial tissue. In contrast, mononuclear cell infiltration and bone and cartilage pathology was absent in sham-MRL/*lpr* mice until age 20 wk.

Recovery of autoimmune arthritis by estrogen administration

The destructive lesions in the knee joints in Ovx-MRL/*lpr* mice were inhibited by estrogen administration (10^{-9} M) at 12 and 20 wk of age (Fig. 2A). Testosterone administration in Ovx-MRL/*lpr* mice resulted in severe inflammatory lesions as the same levels. We confirmed gene expression in ER-α but not ER-β in synovial tissues by RT-PCR analysis (Fig. 2B), indicating that estrogenic action to the synovial tissues might be directly affected through estrogen/ER-α binding *in vivo*. We detected increased levels of serum RF, anti-dsDNA, and anti-CII Abs in Ovx-MRL/*lpr* mice compared with those in sham mice, and these levels were entirely recovered in Ovx-MRL/*lpr* mice that underwent estrogen administration (Fig. 2C).

Effects of the Ovx on cytokine and MMP expression

Culture supernatants from anti-CD3 mAb-stimulated LN T cells obtained from Ovx-MRL/*lpr* mice at 20 wk of age contained high levels of IFN-γ, whereas no difference in levels of IL-2 and IL-4 was observed by ELISA (Fig. 3A). We next analyzed the effects of the Ovx on various gene expressions in the synovial tissues. Increased expressions of cytokine genes including IL-1β, IFN-γ, TNF-α, IL-6, IRF-1, and β-actin mRNA were detected in synovial tissues from Ovx-MRL/*lpr* mice at 20 wk of age, compared with those from sham-MRL/*lpr* mice by RT-PCR analysis (Fig. 3B). In addition, we found elevated gene expressions of MMP-3 and MMP-9 in synovial tissues from Ovx-MRL/*lpr* mice (Fig. 3C). These data suggest that estrogen deficiency induces various gene expressions directly responsible for tissue damage on the development of autoimmune arthritis.

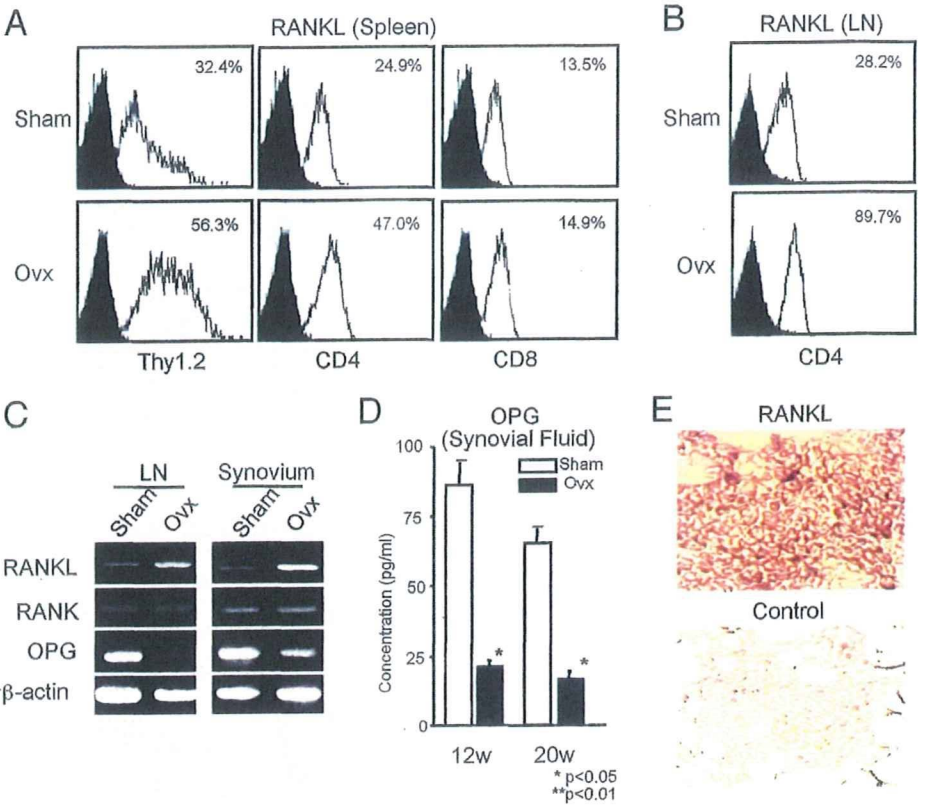

FIG. 4. A significant increase in splenic Thy1.2$^+$ and CD4$^+$ T cells bearing RANKL from Ovx-MRL/lpr mice at 20 wk of age was observed as compared with those from sham-MRL/*lpr* mice, whereas no remarkable change in CD8$^+$ T cells bearing RANKL was found (A). A large proportion of CD4$^+$ T cells in LN bearing RANKL (89.7%) from Ovx-MRL/*lpr* mice was detected on flow cytometry, as compared with that of sham-MRL/*lpr* mice (28.2%) (B). A prominently enhanced RANKL mRNA and an impaired OPG mRNA were observed in LN and synovium from Ovx-MRL/*lpr* mice by RT-PCR analysis (C). A significantly decreased OPG concentration was found in synovial fluid of Ovx-MRL/*lpr* mice at ages 12 (12w) and 20 wk (20w) (*, $P < 0.05$; **, $P < 0.01$, Student's *t* test) (D). A large proportion of infiltrating cells in synovium was positive for RANKL in Ovx-MRL/*lpr* mice at 20 wk of age. Isotype-matched controls were all negative (E).

Effects of the Ovx on RANKL, RANK, and OPG expression

We analyzed the spleen and LN cells bearing RANKL by flow cytometry. A significant increase of Thy1.2$^+$, and CD4$^+$ T cells bearing RANKL in the spleen from Ovx-MRL/*lpr* mice was observed, compared with those from sham-MRL/*lpr* (Fig. 4A). We detected a large proportion of CD4$^+$ T cells in LN bearing RANKL (89.7%) from Ovx-MRL/*lpr* mice as compared with those from sham-MRL/*lpr* mice (28.2%) (Fig. 4B). In addition, an enhanced RANKL mRNA and an impaired OPG mRNA were observed in LN and synovium from Ovx-MRL/*lpr* mice, compared with those in sham-mice by RT-PCR analysis (Fig. 4C). Indeed, a significant decrease in OPG concentration was found in synovial fluid of Ovx-MRL/*lpr* mice compared with those of sham-mice at 12 and 20 wk of age (Fig. 4D). A large proportion of infiltrating cells in synovium was positive for RANKL in Ovx-MRL/*lpr* mice (Fig. 4E).

Effects of the Ovx on OC formation and bone resorption

As seen in Fig. 5A, numerous multinucleated (more than three nuclei), TRAP-positive OC-like cells were detected in the knee joints from both Ovx- and sham-MRL/*lpr* mice. A significant increase in number of OCs formed in the joints from Ovx-MRL/*lpr* mice was observed compared with those from sham-MRL/*lpr* mice (Fig. 5B). We next examined *in vitro* whether the TRAP-positive multinucleated cells (more than three nuclei) from bone marrow cells resorbed bovine bone slices (30). When the bone marrow cells were cultured with dexamethasone and 1α,25-$(OH)_2D_3$, they differentiated into TRAP-positive multinucleated cells, and numerous resorption pits were formed on their surfaces (Fig. 5C). A significantly large number of resorption pits were formed using the bone marrow cells from Ovx-MRL/*lpr* mice compared with those from sham-MRL/*lpr* mice (Fig. 5D).

Discussion

RA is characterized by progressive joint damage that is mediated by several mechanisms (31). Although the etiology of RA remains unknown, joint damage results from the degradation of connective tissue by MMPs and the stimulation of osteoclastogenesis by activated CD4$^+$ T cells (10). Sex hormones influence both humeral and cell-mediated immune response, and estrogen is one of potential factors in this immunological dimorphism (32–34). We have examined the effects of the Ovx on the development of autoimmune arthritis in animals that are susceptible to the development of human RA-like disease. Histology of autoimmune arthritis in Ovx-MRL/*lpr* mice showed severe destructive changes in the younger age examined. It is generally accepted that a severe inflammatory arthritis and systemic autoimmune disease, including glomerulonephritis and autoantibody production, develop in aged (>6-month-old) MRL/*lpr* mice (21, 22). We show here that estrogen deficiency caused a severe inflammatory arthritis in younger (<3-month-old) MRL/*lpr* mice, and these lesions were dramatically prevented by exogenous estrogen treatment. Although the mechanism in detail of estrogen activity still remains unclear, these findings suggest that estrogenic action has an important role during development of autoimmune arthritis in MRL/*lpr* mice. An estrogen deficiency by Ovx in murine RA model results in a significant increase of serum RF, anti-dsDNA Abs, and anti-CII Ab, and these changes were recovered by estrogen ad-

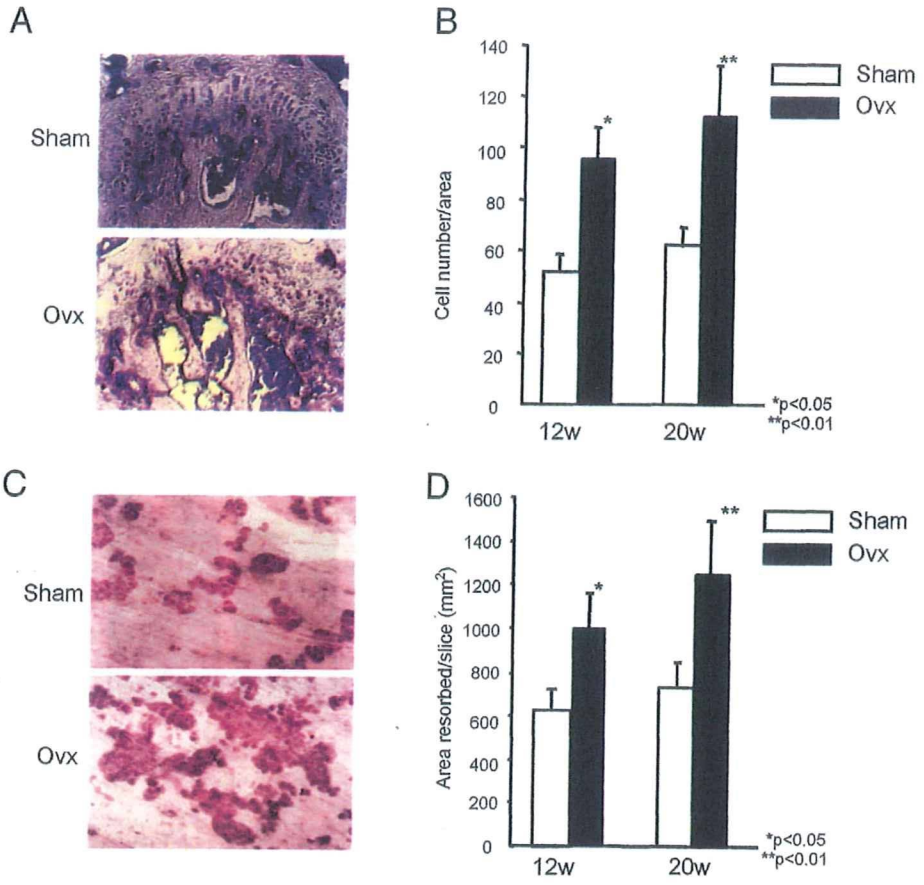

FIG. 5. Effect of the Ovx on OC formation and bone resorption assay. TRAP-positive OC-like cells were detected in the knee joints from both Ovx- and sham-MRL/*lpr* mice (A). A significantly increased number of OCs formed in the joints from Ovx-MRL/*lpr* mice at ages 12 (12w) and 20 wk (20w) was observed compared with those from sham-MRL/*lpr* mice (B) (*, $P < 0.05$ and **, $P < 0.01$, Student's t test). TRAP-positive multinucleated cells (more than three nuclei) from bone marrow cells were observed in both Ovx- and sham-MRL/*lpr* mice when cultured with dexamethasone (10^{-7} M) and $1\alpha,25\text{-}(OH)_2D_3$ (10^{-8} M) (C). A significantly large number of resorption pits was formed using the bone marrow cells from Ovx-MRL/*lpr* mice compared with those from sham-MRL/*lpr* mice (*, $P < 0.05$ and **, $P < 0.01$, Student's t test)(D).

ministration. A previous report has shown that treatment with low doses of β-estradiol exerts a suppressive effect on both development of collagen arthritis as well as T cell-dependent immune reactivity toward type II collagen (35). It was also reported that an estrogen deficiency stimulates B cell development (36) and autoantibody production (36–38), and its increase by an estrogen deficiency has been mediated by cytokines such as IL-6, IFN-γ, and TNF-α (39–41). A recent report has demonstrated that estrogen deficiency induces bone loss by increasing T cell proliferation through IFN-γ-induced class II transactivator (42).

Bone resorption is regulated by the immune system, in which T cell expression of RANKL, which is essential for osteoclastogenesis, may contribute to pathological conditions, such as RA (43). However, it remains unclear whether activated T cells maintain bone homeostasis by counterbalancing the action of RANKL. In this study, a significant increase of $CD4^+$ T cells bearing RANKL in the spleen and inguinal LN from Ovx-MRL/*lpr* mice was observed. Moreover, we detected an enhanced RANKL mRNA expression and $RANKL^+$ infiltrating cells in synovium from Ovx-MRL/*lpr* mice. In contrast, an impaired OPG concentration was found in synovial fluid, in addition to a decreased OPG mRNA in synovium of Ovx-MRL/*lpr* mice. Although molecular mechanisms demonstrating that the appearance of increased RANKL expression in T cells and synovium is related to the development of the autoimmune response are obscure, a role for RANKL in bone resorption in RA is suggested by the identification of RANKL mRNA and protein in cultured synovial fibroblasts from patients with RA and in $CD4^+$ and $CD8^+$ T cells in RA synovial tissues (10). Additional evidence that RANKL plays a critical role in the pathogenesis of bone destruction in inflammatory arthritis comes from studies in the rat adjuvant arthritis model (44, 45). Moreover, it has been recently demonstrated that up-regulation of RANKL on bone marrow cells is an important determinant of increased bone resorption induced by estrogen deficiency (46). Treatment with OPG also prevented OC accumulation, whereas destruction of bone in untreated arthritic animals was accompanied by the accumulation of large numbers of $TRAP^+$ OC-like cells (47). OPG treatment in an animal model of arthritis that is dependent on T cell activation has the potential for blocking not only the effects of RANKL on OC differentiation and activation but also the influence of RANKL on T cell-DC interactions (20).

OCs have a crucial role in the local bone destruction that occurs in association with chronic inflammatory diseases (48). Diseases such as RA have been associated with the accumulation of TNF-α and/or other proinflammatory cytokines such as IL-1 and IL-6, which likely mediate local bone destruction by stimulating OC activity (49). The results in the present study demonstrated an increased gene expression of cytokines including IL-1β, TNF-α, IL-6, IFN-γ, β-actin, and IRF-1 in the synovium from Ovx-MRL/*lpr* mice. In addition, an elevated gene expressions of MMP-3 and MMP-9 mRNA were observed in the synovium. Moreover, we found a significant increase in number of OCs, and bone resorption pits formed in Ovx-MRL/*lpr* mice. It has been shown that estro-